26th International Conference
ENGINEERING MECHANICS 2020
Brno, Czech Republic, November 24 – 25, 2020

ALTERNATIVE STRAIN-RATE DEPENDENT HYPERELASTIC-PLASTIC MATERIAL MODEL

Jerábek R.*, Écsi L.**

Abstract: *At present, multiplicative plasticity-based models are used to model material degradation of hyperelastic materials within the framework of finite-strain elastoplasticity. The underlying theory assumes that the intermediate configuration of the body is locally unstressed, and as a result, no plastic deformation field exists that meets the conditions of compatibility. The assumption is; however, neither mathematically nor physically justified and the related material models are not continuum-based. In this paper, an alternative strain-rate dependent hyperelastic-plastic material model is presented. Based on the theory of nonlinear continuum mechanics for finite deformation of elastoplastic media, the model can describe the plastic flow in an objective and thermodynamically consistent manner. Therefore the strain-rate density of the model and the specimen from the uniaxial tensile test of the modelled material can be related. In this paper, the dynamic behaviour of a silicone cross-shaped specimen is studied numerically using a Mooney-Rivlin material model with internal damping.*

Keywords: Nonlinear continuum theory for finite deformations of elastoplastic media, Objective and thermodynamically consistent formulation, Hyperelastic-plastic material, Mooney-Rivlin material with internal damping.

1. Introduction

Hyperelastic materials, such as natural and synthetic rubber, vulcanized elastomers, various types of polymers, biomaterials and many others are nonlinear elastic materials. The characteristic feature of hyperelastic materials is that they can undergo large elastic deformations without permanent deformations or being damaged. The materials are often considered to be isotropic, and their constitutive functions are derived from strain energy density functions (Hackett, 2018).

At present, hyperelastic-plastic multiplicative plasticity models are used to model material degradation of hyperelastic materials within the framework of finite-strain elastoplasticity. The underlying theory assumes that the intermediate configuration of the body is stress-free (Simo and Hughes, 2000) or locally unstressed (De Souza Neto et al., 2008), for which no plastic deformation field exists that meets the conditions of compatibility. The assumption is; however, neither mathematically nor physically justified, and their related material models are not continuum-based (Écsi et al., 2019b).

The aim of this paper is to present a numerical study on material degradation of a silicone cross-shaped specimen loaded in biaxial tension at various strain rates. In the numerical experiments, an alternate strain-rate dependent hyperelastic-plastic Mooney-Rivlin material model with internal damping has been used. The material model is based on the nonlinear continuum theory for finite deformations of elastoplastic media which allows for the development of objective and thermodynamically consistent material models (Écsi and Élesztős, 2018; 2020). A few selected analysis results are presented and briefly discussed.

2. The stress constitutive function of the material

Écsi and Élesztős (2018; 2020) presented the nonlinear continuum theory for finite deformations of elastoplastic media. The modified Mooney-Rivlin material model, based on this theory, is capable of

* Ing. Róbert Jerábek: Institute of Applied Mechanics and Mechatronics, Faculty of Mechanical Engineering, Slovak University of Technology in Bratislava, Námestie slobody 17; 812 21, Bratislava 1; SR, robert.jerabek@stuba.sk

** Assoc. Prof. Ing. Écsi Ladislav, PhD.: Institute of Applied Mechanics and Mechatronics, Faculty of Mechanical Engineering, Slovak University of Technology in Bratislava, Námestie slobody 17; 812 21, Bratislava 1; SR, ladislav.ecsi@stuba.sk

doi: 10.21495/5896-3-242

imitating material degradation of hyperelastic materials within the framework of finite-strain elastoplasticity. When considering the kinematics of deformation, the theory allows for the separation of the elastic motion from the plastic motion by subtracting the Lagrangian plastic displacement field from the overall Lagrangian displacement field. Then assuming that the body undergoes elastic deformation and then plastic deformation at its every constituent, the elastic part of the deformation gradient, which maps every material point from the initial to the intermediate configuration of the body, can be expressed as:

$$\mathbf{F}^{el} = \mathbf{F} - \frac{\partial^0 \mathbf{u}^{pl}}{\partial \mathbf{X}}. \tag{1}$$

Furthermore, considering that the elastic deformation gradient can multiplicatively be split into a volumetric part $\mathbf{F}_{vol}^{el}$ and an isochoric part $\mathbf{F}_{iso}^{el}$, the left elastic isochoric Cauchy-Green deformation tensor can be expressed in the following form (De Souza Neto et al., 2008 and Hackett, 2018):

$$\mathbf{B}_{iso}^{el} = \mathbf{F}_{iso}^{el} \cdot \left(\mathbf{F}_{iso}^{el}\right)^T = \det\left(\mathbf{F}^{el}\right)^{-\frac{2}{3}} \cdot \mathbf{B}^{el}. \tag{2}$$

The corresponding strain energy density function in the Kirchhoff stress space defined over the intermediate configuration of the body, therefore, remains the same and takes the following form in the case of the compressible Mooney-Rivlin material (Crisfield, 2001 and Hackett, 2018):

$$\overline{\psi}^*\left(I_1^*, I_2^*, J^{el}\right) = C_{10} \cdot \left(I_1^* - 3\right) + C_{01} \cdot \left(I_2^* - 3\right) + \frac{1}{d} \cdot \left(J^{el} - 1\right)^2. \tag{3}$$

Here $I_1^* = I_1^*\left(\mathbf{B}_{iso}^{el}\right)$ and $I_2^* = I_2^*\left(\mathbf{B}_{iso}^{el}\right)$ respectively, are the invariants of the characteristic equation of the associated eigenvalue problem defined by the $\mathbf{B}_{iso}^{el}$ matrix and $J^{el} = \det\left(\mathbf{F}^{el}\right)$ is the Jacobian of elastic deformation. Then material parameters C_{10} and C_{01}, characterizing shear behaviour of the material, and d, which controls bulk compressibility, are material constants (De Souza Neto et al., 2008 and Hackett, 2018). The stress constitutive function of the modified Mooney-Rivlin material then can be expressed as a Kirchhoff stress measure in the intermediate configuration of the body as:

$$\boldsymbol{\tau}^{el} = \frac{\partial \overline{\psi}^*}{\partial \mathbf{F}^{el}} \bullet \left(\mathbf{F}^{el}\right)^T. \tag{4}$$

After carrying out the differentiation, Eqn. (4) can be manipulated into its final form:

$$\boldsymbol{\tau}^{el} = 2\left(C_{10} + C_{01} \cdot I_1^*\right) \cdot dev\left[\mathbf{B}_{iso}^{el}\right] - 2 \cdot C_{01} \cdot dev\left[\left(\mathbf{B}_{iso}^{el}\right)^2\right] + \frac{2}{d} \cdot J^{el} \cdot \left(J^{el} - 1\right) \cdot \mathbf{I}, \tag{5}$$

where $dev\left[\mathbf{B}_{iso}^{el}\right]$ and $dev\left[\left(\mathbf{B}_{iso}^{el}\right)^2\right]$ denote the deviators of the tensors $\mathbf{B}_{iso}^{el}$ and $\left(\mathbf{B}_{iso}^{el}\right)^2$ respectively.

In order to take into account the internal damping, a viscous term was added to the stress constitutive function of the material, which takes the following form in the reference configuration of the body (Jerábek and Écsi, 2019):

$$\mathbf{S} = \mathbf{S}^{el} + \mathbf{S}^{vis} = \left(\mathbf{F}^{el}\right)^{-1} \cdot \boldsymbol{\tau}^{el} \cdot \left(\mathbf{F}^{el}\right)^{-T} + {}^{mat}\mathrm{C}^{vis} : {}^{*}\dot{\mathbf{E}}^{el}. \tag{6}$$

Here $\mathbf{S}^{el}$ is the elastic part, and $\mathbf{S}^{vis}$ is the viscous part of the 2nd Piola-Kirchhoff stress tensor, ${}^{*}\dot{\mathbf{E}}^{el}$ is the material elastic Green-Lagrangian strain-rate tensor (Écsi et al., 2019a) and ${}^{mat}\mathrm{C}^{vis}$ is the fourth-order material viscosity tensor, expressed in the form:

$${}^{mat}\mathrm{C}^{vis} = 2 \cdot G^{vis} \cdot \mathrm{I} \mp \lambda^{vis} \cdot \mathbf{I} \otimes \mathbf{I},\ G^{vis} = \frac{E^{vis}}{2 \cdot \left(1 + \upsilon^{vis}\right)},\ \lambda^{vis} = \frac{\upsilon^{vis} \cdot E^{vis}}{\left(1 + \upsilon^{vis}\right) \cdot \left(1 - 2 \cdot \upsilon^{vis}\right)}, \tag{7}$$

where G^{vis} is the viscous shear modulus, λ^{vis} is the viscous Lamé constant, I and **I** are the symmetric fourth- and second-order identity tensors, E^{vis} is the viscous Young's modulus, and υ^{vis} is the viscous Poisson's ratio.

The final form of the stress constitutive function of the modified Mooney-Rivlin material with internal damping then can be expressed as follows in the current configuration of the body:

$$\boldsymbol{\tau} = \mathbf{F}\cdot\mathbf{S}\cdot\mathbf{F}^{T} = \mathbf{F}\cdot\left[\left(\mathbf{F}^{el}\right)^{-1}\cdot\boldsymbol{\tau}^{el}\cdot\left(\mathbf{F}^{el}\right)^{-T} + {}^{mat}\mathrm{C}^{vis} : {}^{*}\dot{\mathbf{E}}^{el}\right]\cdot\mathbf{F}^{T}. \qquad (8)$$

In our study, we considered J_2 plasticity with isotropic hardening to take into account the plastic flow in the material. The corresponding yield surface was defined in the Kirchhoff stress space in the same way as in (Écsi and Élesztős, 2020).

3. Numerical experiment and results

In our numerical experiment material degradation of a silicone cross-shaped specimen in biaxial tension was studied at various strain rates. The geometry and the material parameters of the specimen were the same as of the one used by the collective Putra et al. (2017) in their real experiment. In the numerical study 1/8 of the FE model was considered employing three planes of symmetry. The biaxial tension was imposed as a prescribed axial velocity acting at the moving ends of the specimen using 0.02 m.s^{-1}, 0.1 m.s^{-1} and 0.2 m.s^{-1} values in every single experiment. The specimen was initially at rest except for the nodes at the specimen moving end, where the prescribed velocities acted. The analyses were run as dynamic until they failed to converge using implicit time integration and a 0.0005 s time step size. Fig. 1 depicts the spatially discretized body of the specimen, where the arrows indicate the prescribed axial velocities.

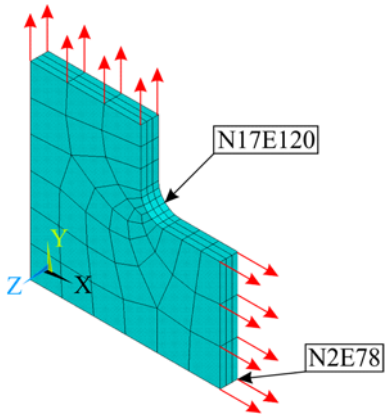

Fig. 1: The spatially discretized specimen.

Tab. 1: Material properties of the specimen.

$\rho_0\ [kg\cdot m^{-3}]$	1 520
$C_{10}\ [Pa]$	114 800
$C_{01}\ [Pa]$	-9 040
$d\ [-]$	0.00000624054
$E^{vis}\ [Pa\cdot s]$	7 310
$\upsilon^{vis}\ [-]$	0.47
${}^{\tau}\tau_y\ [Pa]$	700 000
${}^{\tau}Q\ [Pa]$	100 000
$b\ [-]$	2.0

Tab. 1 outlines the material parameters used in the finite element analysis, where the last three constants are the parameters of the uniaxial Kirchhoff stress-strain curve of the material. Here ${}^{\tau}\tau_y$ is the constant yield stress, ${}^{\tau}Q$ is the maximum hardening stress, and b is the maximum value of the axial plastic strain, at which the material loses its integrity.

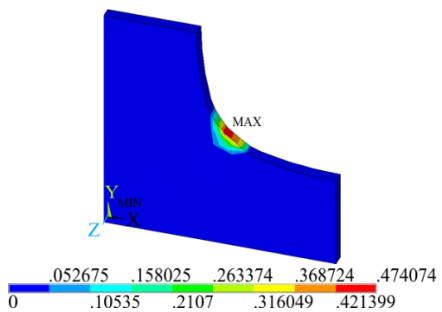

Fig. 2: Accumulated plastic strain distribution [-].

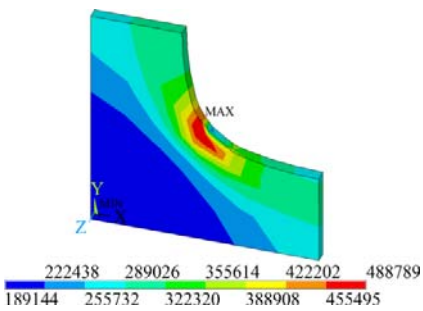

Fig. 3: Von Mises stress distribution [Pa].

The figures above show the accumulated plastic strain and the von Mises stress distribution over the specimen at the end of the analysis using 0.02 m.s^{-1} prescribed axial velocity.

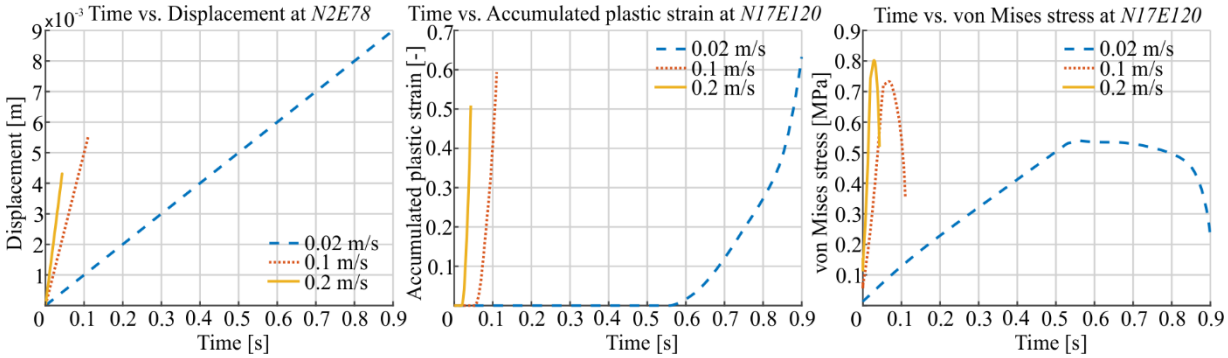

Fig. 4: A few selected time-history curves.

In order to take a more in-depth look at the analysis results, time-history curves of selected variables at nodes N2E78 and N17E120 were created (Fig. 4, see Fig. 1 for the location of the nodes). The figure shows that the greatest axial elongation of the specimen was at 0.02 m.s-1 prescribed velocity. The accumulated plastic strain, which is the measure of material degradation, decreases with increasing values of the prescribed velocity. The maximum value of the von Mises stress, on the other hand, increases with increasing values of the prescribed velocity, while the corresponding plastic work decreases.

4. Conclusions

In this research, an alternative strain-rate dependent hyperelastic-plastic Mooney-Rivlin material model with internal damping has been presented. Based on the nonlinear continuum theory of finite deformations of elastoplastic media, the model enables to characterize material degradation and describe the plastic flow in an objective and thermodynamically consistent manner. The analysis results seem to be reasonable, though proper verification of the material model requires thorough material testing, which still needs to be done.

Acknowledgement

Funding from the Collegium Talentum Programme of Hungary, the VEGA 1/0271/20 grant and the KEGA 017STU-4/2018 grant resources is greatly appreciated.

References

Crisfield, M. A. (2001) Non-linear finite element analysis of solids and structures, Advanced topics, vol. 2. John Wiley & Sons LTD, Chichester.

De Souza Neto, E. A., Perić, D. and Owen, D. R. J. (2008) Computational Methods for Plasticity, Theory and Applications. John Wiley & Sons Ltd., Singapore.

Écsi, L. and Élesztős, P. (2018) An alternative material model using a generalized J2 finite-strain flow plasticity theory with isotropic hardening. Int. J. of Applied Mechanics and Engineering, 23(2), pp. 339-353.

Écsi, L. and Élesztős, P. (2020) An alternative method for modelling the degradation of hyperelastic materials within the framework of finite-strain elastoplasticity. in: Engineering Design Applications II. Advanced Structured Materials (eds. Öchsner, A. and Altenbach H.), Springer. 113, pp. 59-82.

Écsi, L., Élesztős, P., Jerábek, R., Jančo, R. and Hučko, B. (2019a) An alternative framework for developing material models for finite-strain elastoplasticity. in: Advances in Composite Materials Development, IntechOpen. doi: 10.5772/intechopen.85112.

Écsi, L., Jerábek, R., and Élesztős, P. (2019b) A study on the "compatibility assumption" of contemporary multiplicative plasticity models. in: Journal of Mechanical Engineering. 69(2), pp. 15-26.

Hackett, R. M. (2018) Hyperelasticity Primer. 2nd ed. Springer, New York.

Jerábek, R. and Écsi, L. (2019) An alternative Neo-Hookean material model with internal damping for finite-strain elastoplasticity. in: Proc. 57th Conf. on Exp. Stress Analysis, Czech Society for Mechanics, Brno, pp. 160-168.

Putra, K. B., Plott, J. and Shih, A. J. (2017) Biaxial Mooney-Rivlin coefficient of silicone sheet by additive manufacturing. Procedia CIRP, 65, pp. 189-195.

Simo, J. C. and Hughes, T. J. R. (2000) Computational Inelasticity. Springer, New York.